Journal of Neuropathology and Experimental Neurology
Vol. 58, No. 9
September, 1999
pp. 1000–1009

PrP^C Glycoform Heterogeneity as a Function of Brain Region: Implications for Selective Targeting of Neurons by Prion Strains

STEPHEN J. DEARMOND, MD, PHD, YIN QIU, MD, PHD, HENRY SÀNCHEZ, MD, PATRICIA R. SPILMAN, MS, ANNE NINCHAK-CASEY, MD, DARWIN ALONSO, PHD, AND VALERIE DAGGETT, PHD

Abstract. We recently found that deletion of the Asn-linked carbohydrate (CHO) at residue 197 of Syrian hamster (SHa) PrP^C while retaining the CHO at Asn 181 has a profound effect on which population of neurons are targeted for conversion of $SHaPrP^C$ to $SHaPrP^{Sc}$ in transgenic (Tg) mice inoculated with scrapie prions. We hypothesized that selective targeting of neuronal populations is determined by cell-specific differences in the affinity of an infecting PrP^{Sc} (prion) for PrP^C and that the affinity might be modulated by nerve cell-specific differences in PrP^C glycosylation. Here we tested this hypothesis by assessing whether or not each brain region in Syrian hamsters synthesizes different PrP^C glycoforms, as inferred from 2D-gel electrophoresis. Reproducible differences in the number and isoelectric point of PrP^C charge isomers were found as a function of brain region. The results of this study support the hypothesis that the PrP^{Sc} accumulation and the vacuolation pattern phenotypes in the brain are governed by neuron-specific differences in PrP^C glycoforms.

Key Words: Glycoform; Neuronal targeting; Oligosaccharide; Prion; Prion protein; Prion strains; PrP^C.

INTRODUCTION

Investigations of scrapie in inbred mouse strains over 25 years ago showed that the disease phenotype is determined both by the strain of scrapie prion and by host genes (1–6). The phenotypic parameters monitored most frequently include: the failure of transmission of a prion strain from one animal species to another, designated the "host species barrier"; scrapie incubation time, defined as the time from inoculation of a prion strain to the onset of clinical disease; and the neuroanatomic distribution of spongiform degeneration, also designated the "lesion profile." From experiments in transgenic (Tg) mice expressing different PrP constructs, the host species barrier was found to be due to a relatively large difference in the amino acid sequence between PrP^{Sc} comprising the infecting prion, which is determined by the animal from which it was derived, and of PrP^C expressed by the host animal (7, 8). The host factor that determines long and short incubation times in inbred mouse strains are 2 polymorphisms of the *Prnp* gene at codons 108 and 189 that result in synthesis of either PrP^C-A or PrP^C-B (9, 10). These small amino acid sequence differences in the host's PrP^C appear to be sufficient to affect its interaction with PrP^{Sc}, the rate of its conversion to nascent PrP^{Sc} and/or the rate of PrP^{Sc}'s accumulation in the brain. The objective of this study has been to learn more about the molecular and cellular mechanisms underlying the lesion profile.

From the Departments of Pathology (SJD, YQ, HS, PRS) and Neurology (SJD), University of California, San Francisco, California; Department of Neurology (AN-C), University of California, San Diego, California; Department of Medicinal Chemistry (DA, VD), University of Washington, Seattle, Washington.

Correspondence to: Stephen J. DeArmond, MD, PhD, Department of Pathology (Neuropathology), HSW 430, University of California, San Francisco, CA 94143-0506.

The host factors involved in selective targeting of neurons for neurodegeneration by prion strains are still poorly understood. Several lines of evidence indicate that, like the propagation of prions, selective neuronal degeneration is also related to the conversion of PrP^C to PrP^{Sc}. Thus, vacuolar degeneration of neurons and reactive astrocytic gliosis in a brain region follow the local exponential increase in PrP^{Sc} concentration and colocalize precisely with sites of PrP^{Sc} deposition (11–14). (A correlation between mutated PrP and neuropathological changes has not yet been established for familial prion diseases of the Gerstmann-Sträussler-Scheinker syndrome-type because nonamyloid plaque PrP in the neuropil is relatively protease sensitive [15] and because it may have a transmembrane topography that eludes detection [16]). Consistent with the neuroanatomic correlation between sites of vacuolar degeneration and PrP^{Sc} deposition in prion diseases acquired by infection, we and others have found that the neuroanatomic pattern of PrP^{Sc} accumulation in the brain is characteristic of each prion strain and is itself a strain defining phenotypic parameter (13, 17, 18). Propagation of prions and neurodegeneration require synthesis of PrP^C by cells as neither occur in *Prnp* gene knockout mice ($Prnp^{o/o}$ mice) following either acute or chronic exposure to prions (19–21). These observations have led to the unifying hypothesis that the propagation of prions and neurodegeneration in prion diseases are both linked to the conversion of PrP^C to PrP^{Sc}. For the above reasons, we believe that investigation of the mechanisms of differential targeting of neurons by prion strains must begin with our current understanding of the steps involved in the propagation of prions. Considerable evidence, reviewed in part above, indicates that a) PrP^C and PrP^{Sc} have different conformations (22), b) formation of new PrP^{Sc} requires synthesis of PrP^C by the host, c) PrP^C must bind to a host factor, provisionally

designated "protein X," to facilitate binding of PrP^{C} to PrP^{Sc} (23, 24), d) an infecting PrP^{Sc} must bind to PrP^{C} (8, 24, 25), e) the conformation of PrP^{Sc} is replicated in PrP^{C} (26), and f) nerve cell degeneration is caused by local exponential accumulation of PrP^{Sc} (11, 14).

In the context of the above steps, we hypothesized that selective targeting of neuronal populations in the CNS is determined by cell-specific differences in the affinity of PrP^{Sc} for PrP^{C}, which in turn determines brain region differences in the rate of nascent PrP^{Sc} formation. Since PrP^{C} is glycosylated at Asn residues 181 and 197 (27, 28), and Asn-linked oligosaccharide side chains are known to modify the conformation and interaction of glycoproteins (29), it seemed reasonable to postulate that variations in the complex CHOs might alter the size of the energy barrier that must be traversed during formation of PrP^{Sc}. If this is the case, then regional variations in CHO structure could account for formation of PrP^{Sc} in particular areas of the brain. Consistent with these possibilities, we recently found that the pattern of PrP^{Sc} accumulation is profoundly altered in Tg mice expressing glycosylation site mutant PrPs compared with mice expressing wild-type PrP^{C} (30). In the same study, we verified earlier observations that PrP charge isomers in 2D-gels are due to variable sialylation of the Asn-linked CHOs (27, 28, 31). Moreover, the number and pH range of charge isomers from wild-type and glycosylation site mutant Syrian hamster (SHa) PrP^{C} expressed in Tg mice appeared to be different in the hippocampus and cerebellum in support of the hypothesis of brain region heterogeneity of PrP^{C} Asn-linked glycosylation.

The goal of the present study is to comprehensively test whether or not brain regions in Syrian hamsters synthesize different sets of SHaPrP^{C} glycoforms, as inferred from 2D-gel electrophoresis patterns.

METHODS AND MATERIALS

Animals

Syrian golden hamsters were purchased from Charles River Laboratories (Lakeview, NJ). The animals were killed at 6–12 weeks of age by CO_2 asphyxiation.

Regional Brain Dissection

Hamster brains were dissected into 7 regions for measurement of PrP^{C}: hippocampus (Hp), cerebellum (Cb), neocortex (NC), hypothalamus (Hy), thalamus (Th), caudate nucleus (Cd), and septum (S)(14).

Sample Preparation

All samples were homogenized in 9 volumes of lysis buffer (v/w) (9.5M urea, 2% Triton, 2% Ampholyte, 5% β-Mercaptoethanol) at 2,000 rpm with 10 up and 10 down strokes of a teflon pestle (clearance 0.1–0.15 mm) in a 10 ml capacity Potter-Elvehjem tissue grinder. The homogenates were centrifuged at 3,000 × g for 30 min and the supernatants were recentrifuged at 100,000 × g for 60 min at 10 °C. The supernatants were stored at −70°C. Ampholyte (Bio-Lyte ampholytes, Bio-Rad Laboratories) ratios were as follows: Ratio A, BioLyte 3/10: BioLyte 5/7 = 1:2 and Ratio B, BioLyte 3/10:BioLyte 5/8 = 1:4.

One- and Two-dimensional Gel Electrophoresis

Two-dimensional (2-D) gel electrophoresis was performed according to the procedure of O' Farrell with minor modifications (32, 33). In the first dimension, isoelectric focusing (IEF) was accomplished in tube gels 125 mm × 2.4 mm in size. Samples from different brain regions containing approximately equal amounts of PrP^{C}, based on densitometric analysis of Western transfers probed with anti-PrP antibody, were placed onto the tube gels and subjected to 400V for 16 hours followed by 850V for 1 hour. The extruded first-dimension gels were incubated in 62.5 mM Tris-HCl, 2% SDS and 5% β-mercaptoethanol at room temperature for 30 min before storage at −70°C. The frozen first-dimension gels were thawed by brief incubation at 37°C and electrophoresed immediately in the second dimension in 12% acrylamide slab gels (150 × 145 mm and 3 mm thick) as described by Laemmli (34). The pH gradient of isoelectric focusing gels was determined from duplicate gels cut into 5 mm lengths and incubated for 2 hours at room temperature in deionized water. One-dimensional (1-D) gel electrophoresis and Western transfers from 1-D and 2-D gels were performed as previously described (11, 14). Western transfers were immunostained with either the 3F4 mouse monoclonal antibody (mAb) (35), which was raised to SHaPrP 27–30 and recognizes an epitope at residues 109–112, or the 13A5 mouse mAb, also raised to SHaPrP 27–30 and recognizes an epitope at residues 138–144 (36). In our analysis of isoelectric points, we focussed exclusively on full-length PrP^{C} glycoforms whose molecular weights are equal to or greater than 30 kDa (37).

Quantitation and Analysis of Western Transfers

To help equalize the amount of PrP^{C} from each brain region loaded onto gels, the size and intensity of immunostaining of bands on Western transfers were measured using a BioQuant video assisted computer densitometer (integrated optical density measurements). The relative mobility of isoelectric points on the Western transfers were measured manually (see Results).

RESULTS

Relative Concentration of PrP^{C} as a Function of Brain Region

Regional differences in the concentration of PrP^{C} were found when aliquots of homogenates from each brain region containing the same amount of total protein were loaded into the wells of a 1-D gel and electrophoresed (Fig. 1A). The range of differences was from about 75% less PrP^{C} in the caudate nucleus, about 60% less in the cerebellum, and about 15% less in the septum relative to the thalamus, based on the measurement of the integrated optical density of all of the PrP^{C} immunostained bands. A standard curve to estimate PrP^{C} concentration was

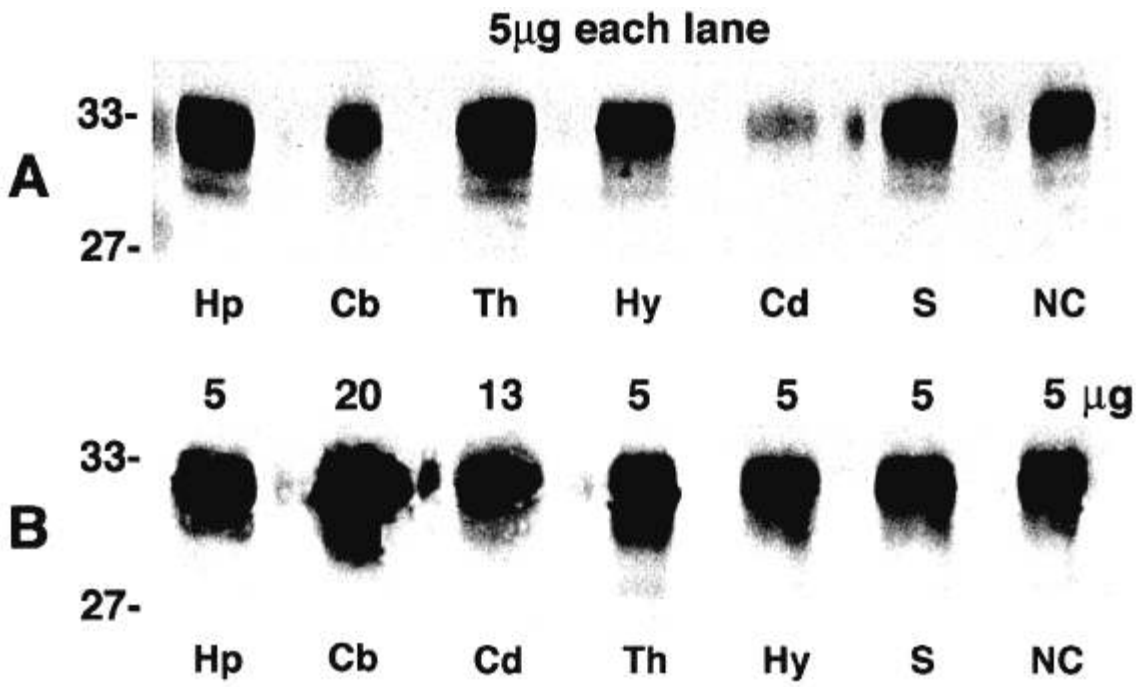

Fig. 1. The relative concentration of PrP^C varies as a function of brain region. A: Aliquots of a 10% homogenate from each brain region containing 5 μg total protein each were loaded into the wells for 1D-electrophoresis. Note that the size and immunostaining intensity of the PrP^C bands from the cerebellum and caudate nucleus in particular are significantly less than other regions. B: Example of an attempt to equalize PrP^C levels among brain regions. Note, loading 20 μg total protein of a cerebellar sample produced a band that was somewhat too large relative to other bands loaded with 5 μg whereas 13 μg for the caudate sample was approximately correct. Both Western transfers were immunostained with the 3F4 mAb. Hp, hippocampus; Cb, cerebellum; Th, thalamus; Hy, hypothalamus; Cd, head of caudate nucleus; S, septum and basal forebrain region; NC, fronto-parietal neocortex.

made from serial dilutions of a hippocampal homogenate as described before (14).

To test whether or not the number of isoelectric points varied as a function of PrP^C concentration, serial dilutions of a hippocampal homogenate were electrophoresed in 2-dimensions and the Western transfer immunostained (Fig. 2). Isoelectric points were typically lost from the acidic side of the array with increasing dilutions. A 50% reduction in the amount of PrP^C loaded relative to the highest concentration loaded resulted in a loss of the ability to detect by eye 1 or 2 of the most acidic isoelectric points on the original Western blot (the loss may appear greater in the photographs). Further reduction in the amount of PrP^C resulted in loss of detection of more acidic isoelectric points. The remaining points appeared to be located at approximately the same locations with slight shifts to the acidic direction. Based on these results, the amount of each sample loaded for each 2D-gel run was adjusted to equalize, as closely as possible, the amount of PrP^C.

To approximate loading equal amounts of PrP^C, particularly from caudate and cerebellum, the relative amount of PrP^C in each brain region was estimated by densitometry of 1-D Western transfers, such as shown in the Figure 1A. Increased amounts of sample total protein were added in an attempt to equalize the size and immunostaining intensity of the PrP^C band relative to the thalamic band (Fig. 1B). Note: loading 20 μg total protein of a cerebellar sample produced a band that was somewhat too large relative to other bands loaded at 5 μg whereas 13 μg of a caudate sample was approximately correct.

Regional Differences in the Number and Location of PrP^C Isoelectric Points

With the total protein content of homogenate adjusted to equalize the amount of PrP^C from each region, differences in the number and locations of PrP^C isoelectric points could be identified by visual inspection (Fig. 3). To determine whether or not the isoelectric pattern for a brain region was reproducible and unique between experimental runs and among different groups of animals, homogenates from 2 to 4 groups of hamsters were compared using the 2 ampholyte ratios. The greatest number of comparisons were made for the neocortex, hippocampus, and cerebellum because there were sufficient quantities of homogenate from these regions to perform multiple electrophoresis runs (Fig. 4). The hippocampus consistently displayed more acidic isoelectric points than

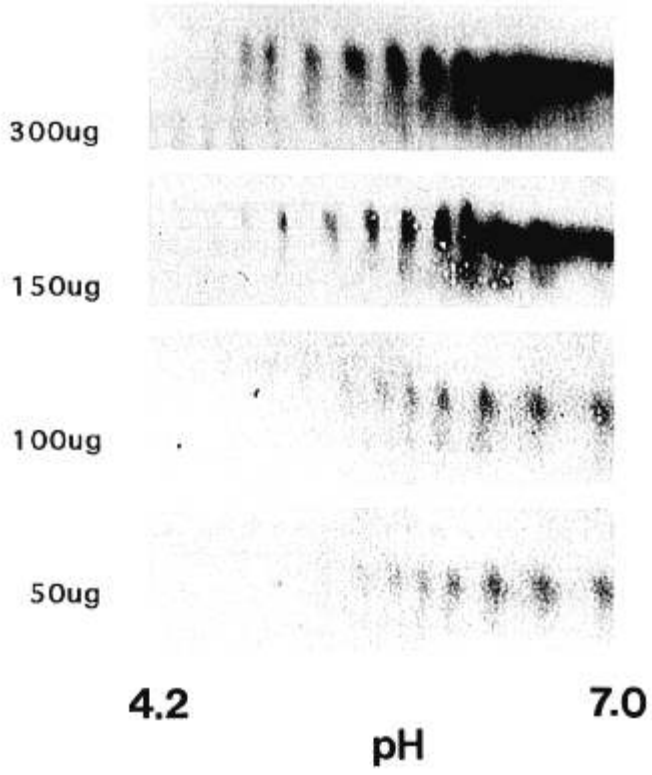

Fig. 2. Progressively fewer hippocampal PrP^{C} isoelectric points are found at lower pH values with decreasing amounts of total protein loaded. The amount of total protein added is indicated. Western transfer immunostained with the13A5 mAb.

either the cerebellum or neocortex regardless of the animal group from which the tissue was pooled or the ampholyte ratio used. No isoelectric points were found more alkaline than pH 7.4 to 7.5 (Figs. 3, 4).

To assemble all of the data from multiple electrophoresis runs and from multiple animal groups into a single graph, the isoelectric points from each run were normalized by choosing 1 spot which could be recognized and whose pH was known. An isoelectric point between pH 5.8–5.9 was present in each run and animal group and served this purpose well for the 2 ampholyte ratios used in this study. The distance to that spot from the alkaline end of each electrophoresis pattern was measured and the fractional distance travelled by other spots calculated (relative isoelectric mobility) (Fig. 5). Analysis of isoelectric points in this way revealed patterns common to each brain region, as well as differences. The isoelectric point at pH 5.8–5.9 was located between another more acidic point and 2 more alkaline points. These 4 isoelectric points and the spacing between them were similar in all brain regions, including those not shown in Figure 5. Differences that distinguished each brain region were on both the acidic and alkaline side of the 4 points. The more acidic isoelectric points resolved into distinct spots whereas the more alkaline points between pH 6.3 and 7.3

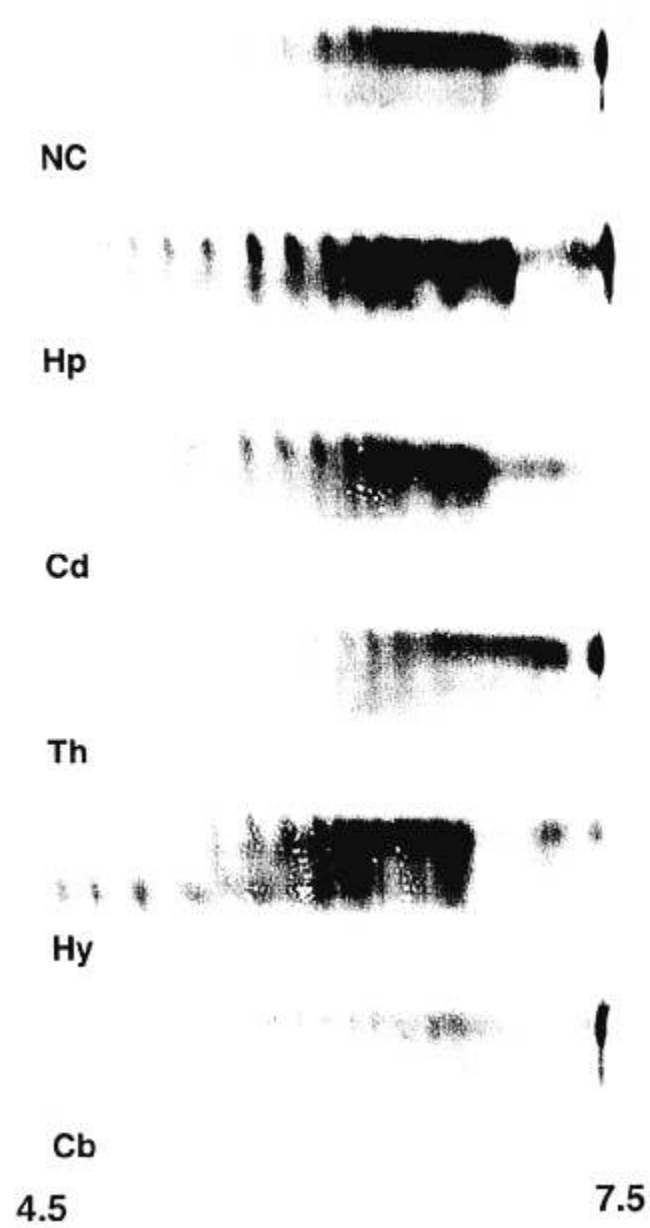

Fig. 3. Differences in the PrP^{C} isoelectric point patterns from 6 brain regions are readily detectable by visual inspection of Western transfers immunostained with the 3F4 mAb. Equal amounts of PrP^{C} from each region were analyzed. Approximate pH range is indicated at bottom. Hp, hippocampus; Cb, cerebellum; Th, thalamus; Hy, hypothalamus; Cd, head of caudate nucleus; S, septum and basal forebrain region; NC, fronto-parietal neocortex.

tended to merge together. The latter was particularly characteristic of the neocortex.

The isoelectric point patterns from multiple runs were consistently different for the neocortex, hippocampus, and cerebellum. Most of the isoelectric points were present in each run (constant points); however, a few isoelectric points were found in some runs but not others (nonconstant points) (Fig. 5). For ampholyte ratio A, the

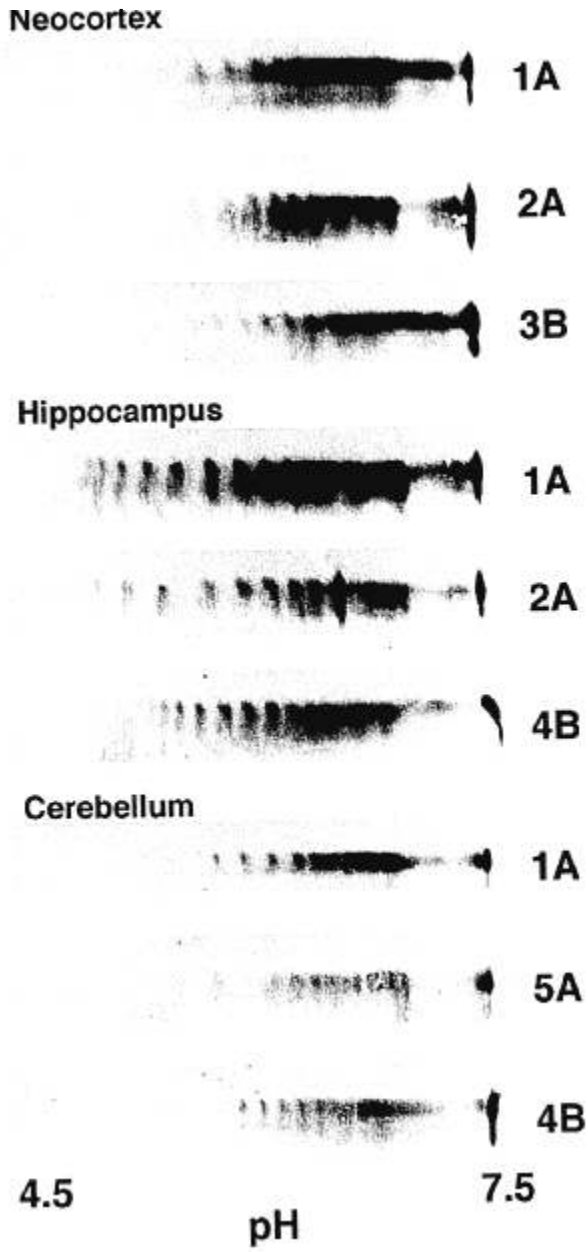

Fig. 4. Brain region differences in PrP^C isoelectric patterns are reproducible among different groups of animals and with 2 different ampholyte ratios. Numbers identify the animal group from which the brain region homogenate was obtained. The letters A and B indicate 2 different ampholyte ratios. Western transblots were immunostained using the 3F4 mAb. The pH range is indicated at the bottom.

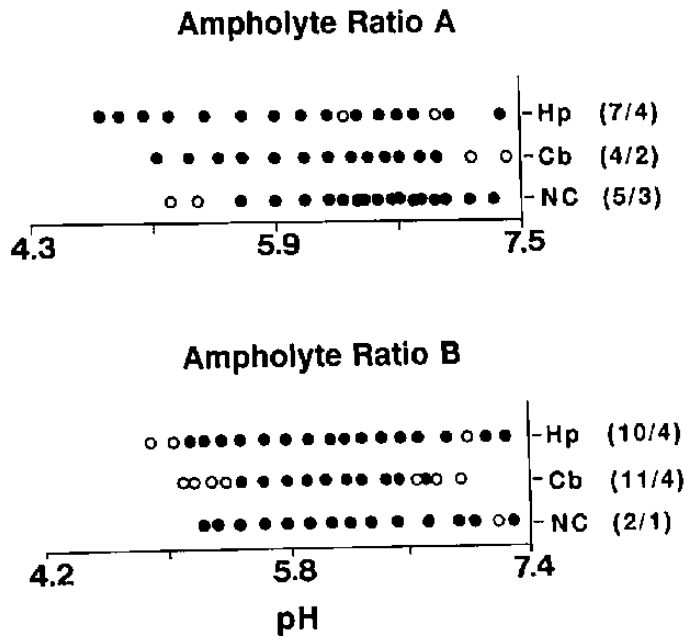

Fig. 5. Graphic summary of multiple electrophoresis runs for the neocortex (NC), hippocampus (Hp), and cerebellum (Cb). Isoelectric points, which appeared in every run from each group of animals, are represented by solid circles and those that failed to occur in 1 or more runs are represented by open circles. The number of electrophoresis runs (left hand number) and the number of animal groups studied (right hand number) are indicated in parentheses.

hippocampus had 15 constant isoelectric points ranging in pH from 4.80 to 7.36 (N = 7) whereas the cerebellum had 13 ranging from pH 5.15 to 7.33 (N = 4). For ampholyte ratio B, the hippocampus had 16 constant isoelectric points from pH 5.18 to 7.25 (N = 10) and the cerebellum, 10 constant points from pH 5.51 to 6.75 (N = 11). 2D-gel runs of neocortical homogenates from 3 groups of animals were different than both the hippocampal and cerebellar patterns, particularly with ampholyte ratio A (Figs. 4, 5). One striking difference was the number of constant isoelectric points between pH 6.1 and 7.1 which was estimated to be 12 for the neocortex, 7 for the hippocampus (plus 2 inconstant points), and 8 for the cerebellum. These results argue that the majority of isoelectric points are reproducible from run to run and between animals and are, therefore, characteristic of a brain region.

DISCUSSION

The results of this study show heterogeneity of PrP^C charge isomers as a function of brain region. Moreover, because our earlier study (30), and those of others (27, 28, 31), found that virtually all of PrP^C's isoelectric points originate from its 2 Asn-linked CHOs, the charge heterogeneity suggests there are reproducible brain region differences in the structure of PrP^C's CHOs. Cell-type-specific glycosylation patterns are well known for other glycoproteins, such that they are referred to as a cell's "glycotype" (38). The results with PrP^C are, therefore, consistent with what is known about cell-specific characteristics of other glycoproteins. Finding PrP^C glycotype variations as a function of brain region is consistent with

our hypothesis that selective targeting of neurons in prion diseases is modulated, at least in part, by PrP^{C}'s CHOs.

Because we analyzed PrP^{C} from dissected brain regions, the spectrum of glycoforms in each most likely represents the products of multiple nerve cell types. Whether the PrP^{C} located in a neuroanatomically defined brain region is synthesized by resident neurons, whether it is carried into the region by axonal transport from neurons outside of the region, or both, is unknown. It is reasonable to assume that glial and endothelial cells in each region contribute little to the set of glycoforms since they express less than 3 PrP mRNAs per cell, whereas neurons express from 10 to 50 depending on the nerve cell type (39). Although prion strains can be identified by reproducible differences in the neuroanatomic pattern of PrP^{Sc} deposition, it is also true that many prion strains target the same brain regions for conversion of PrP^{C} to PrP^{Sc} (13, 17, 18). If indeed PrP^{C}'s Asn-linked CHOs modulate its interaction with PrP^{Sc}, finding only minor differences in the isoelectric point patterns among some brain regions may explain why the same brain regions are targeted by different prion strains.

How might Asn-linked oligosaccharides influence PrP^{C}'s interaction with PrP^{Sc} and be the basis of selective neuronal targeting? One possibility is that the flexibility and/or conformation of that portion of the PrP^{C} molecule that interacts with PrP^{Sc} and whose conformation is changed during conversion to nascent PrP^{Sc} is influenced by variations in PrP^{C}'s CHOs. The PrP molecule has 2 domains that play different roles in the conversion of PrP^{C} to PrP^{Sc} (Fig. 6). First, there is a "stable" or "ordered" core domain that contains the 2 Asn-linked oligosaccharides; 2 α-helices, designated helix-B and helix-C, that are stabilized by a disulfide bridge between Cys^{179} and Cys^{214}; the phosphatidylinositol glycolipid (GPI) attached to the C-terminus at residue 231 which anchors PrP^{C} to the plasma membrane; and the protein X binding sites, which are believed to lower the energy barrier for conversion of PrP^{C} to PrP^{Sc} when PrP^{C} binds to protein X (23, 24). Secondly, there is a "variable" or "disordered" domain that contains the portion of the molecule that interacts with PrP^{Sc} and changes its conformation from primarily unstructured in PrP^{C} to β-sheet in PrP^{Sc} (40). Nuclear magnetic resonance (NMR) and nuclear Overhauser effect (NOE) spectroscopy of 2 large synthetic PrP fragments, PrP 90-231 (41) and PrP 29-231 (42), suggest that the variable domain of PrP^{C} is largely unstructured; however, it does contain a relatively short α-helix (helix-A, residues 144–156) and 2 short antiparallel β-strands (residues 129–131 and 161–163). Investigations of the steps required for prion propagation and neurodegeneration in Tg mice expressing chimeric mouse-hamster-mouse or mouse-human-mouse PrP transgenes indicate that residues 90–140 in the variable region play a particularly important role in the interaction of PrP^{C} with PrP^{Sc} leading to the conversion of the former to the latter (24, 25). Residues 90–140 are largely unstructured or weakly helical in PrP^{C} (41, 42) but are predicted to be β-sheet in PrP^{Sc} (40). In addition, helix A may be converted to β-sheet along with other portions of the variable region during the conversion to PrP^{Sc}. Consistent with these possibilities, Fourier transform infrared and circular dichroism spectroscopy indicate that PrP^{C} contains about 40% α-helix and about 3% β-sheet whereas PrP^{Sc} contains about 30% α-helix and 45% β-sheet (22).

Several lines of evidence indicate that Asn-linked CHOs influence protein conformation (29). For example, Asn-linked glycosylation was found to cause a hemagglutinin peptide to adopt a more compact, folded conformation (43). Glycosylation of epitopes in the rabies virus glycoprotein was found to disrupt α-helical structure and to induce formation of a β-turn; moreover, the "most dramatic effects" occurred on addition of a single, simple carbohydrate (44). The latter raises the possibility that some PrP^{C} glycoforms may more readily convert to PrP^{Sc} than others. Glycosylation appears to influence disulfide bridges between serum IgM peptides, possibly by reducing the mobility of the peptide tailpieces (45). Glycosylation of a highly conserved 15-residue loop region in the nicotinic acetylcholine receptor facilitates disulfide bridge formation apparently by bringing the termini of the loop into closer proximity (46). In some cases, such as the CD2 receptor of T-cells, the oligosaccharide binds to a positively charged cluster of 5 solvent-exposed lysine residues that destabilize the functionally relevant conformation in the deglycosylated molecule (47, 48). With regard to the influence of oligosaccharides on specific targeting of cells, a single carbohydrate residue difference among cell surface antigens determines whether or not E. coli targets the urinary tract for infection (49). The foregoing provide precedent for the idea that the CHOs may influence the conformation and flexibility of residues 90–140 in the PrP^{C} molecule.

The location of the protein X binding sites on adjacent portions of helices B and C, to which the CHOs are attached, raises the intriguing possibility that protein X may facilitate the interaction of PrP^{Sc} with PrP^{C} by adjusting the CHO's position relative to the variable half of the PrP^{C} molecule. Consistent with this possibility, exposure of scrapie-infected N2a cells in vitro to tunicamycin, which prevents glycosylation of nascent PrP^{C}, does not prevent PrP^{Sc} formation (50). Whether unglycosylated PrP^{C} is more rapidly converted to PrP^{Sc} in ScN2a cells was not determined. In the context of these findings, we believe that PrP^{C}'s CHOs may tend to impede its conversion to PrP^{Sc}, that the degree of the effect on conversion is a function of the structure of PrP^{C}'s

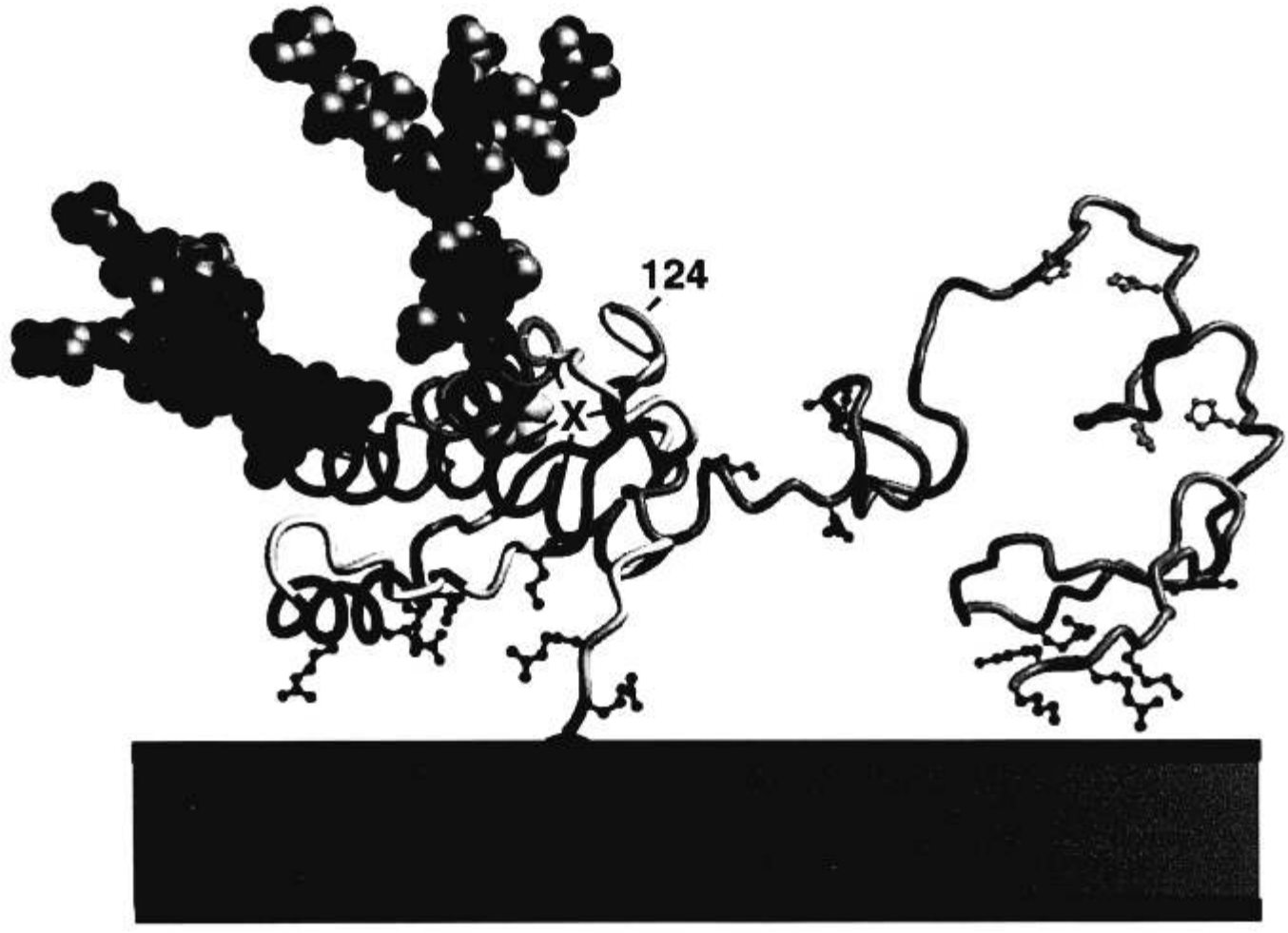

Fig. 6. Structural model of the SHaPrP^{C} molecule. The purpose of the model is to depict the relative sizes of and locations of the Asn-linked oligosaccharides relative to the published structure of SHaPrP fragments inferred from NMR spectroscopy (41, 42). SHaPrP^{C} is shown attached to the plasma membrane by its GPI anchor to indicate how the range of movement of the N-terminal half of the molecule might be constrained in vivo. The model also shows the location of positively charged Lys and Arg residues (blue). Those located along the plasma membrane surface of the molecule have the potential to interact with negative charges on the plasma membrane surface. Those located in the flexible N-terminal half of the molecule have the potential to interact with negatively charged sialic acid residues in the CHOs. A growing body of evidence suggests that the normal physiological role of PrP^{C} is to store and present copper to cells (65). Recombinant SHaPrP(29–231) binds 2 Cu^{++} molecules to His residues in the octarepeat region near the N-terminus and, in doing so, brings about a conformational change (66). The more **ordered** portion of the molecule, residues 125–231, contains helices A (red, residues 144–157), B (green, residues 172–193) and C (blue, 200–227). The disulfide bridge linking Cys^{179} of helix B with Cys^{214} of helix C is shown (yellow, space filling group). The Asn-linked CHO at residue 181, which is attached to helix B, and the CHO at Asn 197, which is on the bridging peptide between helix B and C, are displayed and represent the predominant defucosylated moieties present in PrP^{Sc} reported by Endo et al. (27). The 2 short anti-parallel β-strands are shown in red (S1, 129–131 and S2, 161–163). The putative protein X binding sites are indicated with an 'X' with lines pointing to the discontinuous epitope on helices C and B with which it interacts (23). The **disordered** portion of the molecule, residues 23–124 (orange), was modeled in a random conformation; however, constraints were applied to the putative Cu^{++} binding His residues (green) to bring them into proximity. The alignment of the His residues was accomplished using an in-house version of the program ENCAD (67) and the Levitt et al force field (68). The Cα-Cα and Nε-Nε distances between His 61 and 69 and between His 77 and 85 were targeted. Since the exact Cu^{++} binding geometry of PrP is unknown, the Nε-Nε distances were allowed to be larger (5.5 Å) than those of the copper binding protein azurin (3.2 Å). The GPI anchor attachment to the plasma membrane is shown schematically.

CHOs, and that PrP^{C}'s CHOs are not necessary for conversion as long as PrP^{C} is in a cellular compartment where it can interact with an infecting PrP^{Sc}.

Given the evidence that each neuron population synthesizes PrP^{C} with a different complement of CHOs and the fact that each prion strain targets a different set of neurons for conversion of PrP^{C} to PrP^{Sc}, one would predict that PrP^{Sc} glycoforms are also prion strain specific. To date, no laboratory has compared PrP^{Sc} isoelectric patterns for different strains of prions. However, different

proportions of di-, mono- and non-glycosylated PrP 27-30 (the proteinase K digestion product of PrP^{Sc}) have been found to characterize different human and animal prion strains. For example, a preponderance of diglycosylated PrP 27-30 has been found by Western analysis in the CNS of patients with new variant CJD of Great Britain compared with most sporadic and iatrogenic CJD cases (51, 52). Similarly, the proportions of unglycosylated to heavily glycosylated PrP 27–30 following passage of prions in mice are sufficiently different to differentiate 7 scrapie prion strains (53).

In animal models of scrapie, the vast majority of PrP^{C} molecules that are converted to PrP^{Sc} are most likely doubly glycosylated because deletion of both CHOs or deletion of the CHO at Asn 181 alone results in retention of PrP^{C} in the cell body, failure of PrP^{C} transport to the plasma membrane of neuritic processes and rapid degradation of PrP^{C} (30). Lehmann and Harris (54) found that MoPrP^{C} in Chinese hamster ovary cells mutated to delete the CHO at Asn 180 alone or to delete both CHOs at Asn 180 and Asn196 failed to reach the cell surface after synthesis; in contrast, both wild-type MoPrP^{C} synthesized in the presence of tunicamycin or mutated MoPrP^{C} in which the CHO at Asn 196 alone was deleted were detected on the plasma membrane. These results suggest that the CHO at Asn 181 in SHaPrP (or at Asn 180 in the case of MoPrP) is particularly important for trafficking of PrP^{C} to the plasma membrane in general and to neuritic processes of neurons in particular. In this regard, PrP^{C} must reach the cell surface prior to conversion to PrP^{Sc} since blocking PrP^{C} export from the ER-Golgi complex to the plasma membrane inhibits formation of PrP^{Sc} (55) and since exposure of scrapie-infected cells to phosphatidylinositol-specific phospholipase C, which releases PrP^{C} from the cell surface, also inhibits formation of PrP^{Sc} (56). Current evidence suggests that PrP^{C} is converted to PrP^{Sc} in caveolae-like domains of the plasma membrane (57). Although PrP^{C} that is mono-glycosylated at Asn 181 (CHO at 197 deleted) is transported to the plasma membrane, it is unlikely that a significant amount of it accumulates as nascent PrP^{Sc}. Thus, while Asn 181 monoglycosylated PrP^{C} has a normal distribution and concentration in the brain that is similar to wild-type PrP^{C}, it requires over 500 days for conversion to PrP^{Sc}, which is more than 3 times as long as the time to death in the animals expressing wild-type PrP^{C} (30).

All of the above observations argue that the variable, but significant, proportions of mono- and non-glycosylated PrP^{Sc} that are characteristic of each prion strain are probably formed after PrP^{C} is converted to PrP^{Sc}. Postconversion modification of PrP^{Sc}'s CHOs is likely because PrP^{Sc}'s peptide component is highly protease resistant while its CHOs, like those of other plasma membrane glycoproteins, will tend to be relatively sensitive to glycosidases (58, 59). CHO degradation may occur in lysosomes where a substantial proportion of PrP^{Sc} becomes stored (55, 60) or PrP^{Sc} molecules may be partially or completely deglycosylated by recycling through nonlysosomal endocytic compartments (61). What then is the relationship of neuroanatomic site of formation of PrP^{Sc} to the origin of prion strain specific proportions of di-, mono- and non-glycosylated PrP^{Sc}? It may be that some brain region-specific PrP^{Sc} glycoforms are preferentially trafficked to cellular compartments where CHOs are digested. Furthermore, some PrP^{Sc} glycoforms may be more easily degraded than others. With regard to the last possibility, degradation of renin glycoforms by the liver is directly related to the proportion of acidic isoelectric points (62). Alternatively, there may be significant differences in the rate or specificity of CHO digestion among neuron populations.

In summary, by viewing prion diseases from the perspective of the neuropathological changes, we have learned that host-determined variations in PrP^{C} play as important a role in determining the disease phenotype as the conformation of PrP^{Sc} comprising an infecting prion. We believe the role of PrP^{C} in the pathogenesis of prion diseases cannot be overemphasized. Indeed, the critics of the "protein only" hypothesis often argue that an infectious agent composed solely of a single abnormally folded protein cannot encode all the information necessary to account for the known variations in the prion disease phenotype. In this they are probably correct because there are most likely only a limited number of different stable strain determining conformations of PrP^{Sc} possible, excluding contributions of PrP^{Sc}'s CHOs. However, these critics do not differentiate between coding of strain information in prions and the combination of both prion and host factors that generate the disease phenotype. The results of this study, as well as others reviewed above, indicate there are more than sufficient animal species-determined variations in the amino acid sequence of PrP^{C}, the level of expression of PrP^{C}, and the CHO structure of PrP^{C} in combination with variations in the conformation and amino acid sequence of PrP^{Sc} to account for all of the known variations in the prion disease phenotype. Other host factors may also influence the disease phenotype, such as the response of microglia or astrocytes (63, 64); nevertheless, all of the evidence indicates that PrP^{C} is the pre-eminent host factor.

ACKNOWLEDGMENTS

This work was dependent on animal resources from a collaboration with the Stanley Prusiner Laboratory and was supported by grants from the National Institutes of Health (AG02132, AG10770, and NS14069) as well as gifts to Stanley Prusiner's Laboratory from the Sherman Fairchild Foundation, the G. Harold and Leila Y. Mathers Foundation, and Centeon.

REFERENCES

1. Dickinson AG, Meikle VMH, Fraser H. Identification of a gene which controls the incubation period of some strains of scrapie agent in mice. J Comp Pathol 1968;78:293–99
2. Dickinson AG, Meikle VMH. Host-genotype and agent effects in scrapie incubation: Change in allelic interaction with different strains of agent. Mol Gen Genet 1971;112:73–79
3. Fraser H, Dickinson AG. The sequential development of the brain lesions of scrapie in three strains of mice. J Comp Pathol 1968;78: 301–11
4. Fraser H, Dickinson AG. Scrapie in mice. Agent-strain differences in the distribution and intensity of grey matter vacuolation. J Comp Pathol 1973;83:29–40
5. Fraser H. Neuropathology of scrapie: The precision of the lesions and their diversity. In: Prusiner SB, Hadlow WJ, eds. Slow transmissible diseases of the nervous system, Vol. 1. New York: Academic Press, 1979:387–406
6. Bruce ME, McConnell I, Fraser H, Dickinson AG. The disease characteristics of different strains of scrapie in *Sinc* congenic mouse lines: Implications for the nature of the agent and host control of pathogenesis. J Gen Virol 1991;72:595–603
7. Prusiner SB, Scott M, Foster D, et al. Transgenetic studies implicate interactions between homologous PrP isoforms in scrapie prion replication. Cell 1990;63:673–86
8. Scott M, Foster D, Mirenda C, et al. Transgenic mice expressing hamster prion protein produce species-specific scrapie infectivity and amyloid plaques. Cell 1989;59:847–57
9. Carlson GA, Kingsbury DT, Goodman PA, et al. Linkage of prion protein and scrapie incubation time genes. Cell 1986;46:503–11
10. Westaway D, Goodman PA, Mirenda CA, McKinley MP, Carlson GA, Prusiner SB. Distinct prion proteins in short and long scrapie incubation period mice. Cell 1987;51:651–62
11. DeArmond SJ, Mobley WC, DeMott DL, Barry RA, Beckstead JH, Prusiner SB. Changes in the localization of brain prion proteins during scrapie infection. Neurology 1987;37:1271–80
12. DeArmond SJ, Prusiner SB. The neurochemistry of prion diseases. J Neurochem 1993;61:1589–601
13. Hecker R, Taraboulos A, Scott M, et al. Replication of distinct prion isolates is region specific in brains of transgenic mice and hamsters. Genes Dev 1992;6:1213–28
14. Jendroska K, Heinzel FP, Torchia M, et al. Proteinase-resistant prion protein accumulation in Syrian hamster brain correlates with regional pathology and scrapie infectivity. Neurology 1991;41:1482–90
15. Hsiao KK, Groth D, Scott M, et al. Serial transmission in rodents of neurodegeneration from transgenic mice expressing mutant prion protein. Proc Natl Acad Sci USA 1994;91:9126–30
16. Hegde RS, Mastrianni JA, Scott MR, et al. A transmembrane form of prion protein in neurodegenerative disease. Science 1998;279: 827–34
17. Bruce ME, McBride PA, Farquhar CF. Precise targeting of the pathology of the sialoglycoprotein, PrP, and vacuolar degeneration in mouse scrapie. Neurosci Lett 1989;102:1–6
18. DeArmond SJ, Yang S-L, Lee A, et al. Three scrapie prion isolates exhibit different accumulation patterns of the prion protein scrapie isoform. Proc Natl Acad Sci USA 1993;90:6449–53
19. Brandner S, Isenmann S, Raeber A, et al. Normal host prion protein necessary for scrapie-induced neurotoxicity. Nature 1996;379:339–43
20. Büeler H, Aguzzi A, Sailer A, et al. Mice devoid of PrP are resistant to scrapie. Cell 1993;73:1339–47
21. Prusiner SB, Groth D, Serban A, et al. Ablation of the prion protein (PrP) gene in mice prevents scrapie and facilitates production of anti-PrP antibodies. Proc Natl Acad Sci USA 1993;90:10608–12
22. Pan K-M, Baldwin M, Nguyen J, et al. Conversion of α-helices into β-sheets features in the formation of the scrapie prion proteins. Proc Natl Acad Sci USA 1993;90:10962–66
23. Kaneko K, Zulianello L, Scott M, et al. Evidence for protein X binding to a discontinuous epitope on the cellular prion protein during scrapie prion propagation. Proc Natl Acad Sci USA 1997;94: 10069–74
24. Telling GC, Scott M, Mastrianni J, et al. Prion propagation in mice expressing human and chimeric PrP transgenes implicates the interaction of cellular PrP with another protein. Cell 1995;83:79–90
25. Scott M, Groth D, Foster D, et al. Propagation of prions with artificial properties in transgenic mice expressing chimeric PrP genes. Cell 1993;73:979–88
26. Cohen FE, Pan K-M, Huang Z, Baldwin M, Fletterick RJ, Prusiner SB. Structural clues to prion replication. Science 1994;264:530–31
27. Endo T, Groth D, Prusiner SB, Kobata A. Diversity of oligosaccharide structures linked to asparagines of the scrapie prion protein. Biochemistry 1989;28:8380–88
28. Haraguchi T, Fisher S, Olofsson S, et al. Asparagine-linked glycosylation of the scrapie and cellular prion proteins. Arch Biochem Biophys 1989;274:1–13
29. O'Connor SE, Imperiali B. Modulation of protein structure and function by asparagine-linked glycosylation. Chem Biol 1996;3: 803–12
30. DeArmond SJ, Sanchez H, Qiu Y, et al. Selective neuronal targeting in prion diseases. Neuron 1997;19:1337–48
31. Bolton DC, Meyer RK, Prusiner SB. Scrapie PrP 27-30 is a sialoglycoprotein. J Virol 1985;53:596–606
32. O'Farrell PH. High resolution two-dimensional electrophoresis of proteins. J Biol Chem 1975;250:4007–21
33. O'Farrell PZ, Goodman HM, O'Farrell PH. High resolution two-dimensional electrophoresis of basic as well as acidic proteins. Cell 1977;12:1133–42
34. Laemmli UK. Cleavage of structural proteins during the assembly of the head of bacteriophage T-4. Nature 1970;227:680–85
35. Kascsak RJ, Rubenstein R, Merz PA, et al. Mouse polyclonal and monoclonal antibody to scrapie-associated fibril proteins. J Virol 1987;61:3688–93
36. Barry RA, Prusiner SB. Monoclonal antibodies to the cellular and scrapie prion proteins. J Infect Dis 1986;154:518–21
37. Pan K-M, Stahl N, Prusiner SB. Purification and properties of the cellular prion protein from Syrian hamster brain. Protein Sci 1992;1:1343–52
38. Rademacher TW, Parekh RB, Dwek RA. Glycobiology. Annu Rev Biochem 1988;57:785–838
39. Kretzschmar HA, Prusiner SB, Stowring LE, DeArmond SJ. Scrapie prion proteins are synthesized in neurons. Am J Pathol 1986;122:1–5
40. Prusiner SB, Scott MR, DeArmond SJ, Cohen FE. Prion Protein Biology. Cell 1998;93:337–48
41. James TL, Liu H, Ulyanov NB, et al. Solution structure of a 142-residue recombinant prion protein corresponding to the infectious fragment of the scrapie isoform. Proc Natl Acad Sci USA 1997;94: 10086–91
42. Donne DG, Viles JH, Groth D, et al. Structure of the recombinant full-length hamster prion protein PrP(29-231): The N terminus is highly flexible. Proc Natl Acad Sci USA 1997;94:13452–57
43. Imperiali B, Rickert KW. Conformational implications of asparagine-linked glycosylation. Proc Natl Acad Sci U S A 1995;92:97–101
44. Otvos L, Thurin J, Kollat E, Urge L, Mantsch HM, Hollosi M. Glycosylation of synthetic peptides breaks helices. Int J Pept Protein Res 1991;38:476–82
45. Wormald MR, Dwek RA. The conformational effects of N-glycosylation on the tailpiece from serum IgM. Eur J Biochem 1991;198: 131–39
46. Rickert KW, Imperiali B. Analysis of the conserved glycosylation site in the nicotinic acetylcholine receptor: Potential roles in complex assembly. Chemistry and Biology 1995;2:751–59

47. Davis SJ, Davies EA, Barclay AN, et al. Ligand binding by the immunoglobulin superfamily recognition molecule CD2 is glycosylation-independent. J Biol Chem 1995;270:369–75
48. Jones EY, Davis SJ, Williams AF, Harlos K, Stuart DI. Crystal structure at 2.8. A resolution of a soluble form of the cell adhesion molecule CD2. Nature 1992;360:232–39
49. Lindstedt R, Larson G, Falk P, Jodal U, Leffler H, Svanborg C. The receptor repertoire defines the host range for attaching Escherichia coli strains that recognize globo-A. Infect Immun 1991;59:1086–92
50. Taraboulos A, Rogers M, Borchelt DR, et al. Acquisition of protease resistance by prion proteins in scrapie-infected cells does not require asparagine-linked glycosylation. Proc Natl Acad Sci USA 1990;87:8262–66
51. Collinge J, Sidle K, Meads J, Ironside J, Hill A. Molecular analysis of prion strain variation and the aetiology of 'new variant' CJD. Nature 1996;383:685–90
52. Hill AF, Desbruslais M, Joiner S, et al. The same prion strain causes vCJD and BSE. Nature 1997;389:448–50
53. Somerville RA, Chong A, Mulqueen OU, Birkett CR, Wood SCER, Hope J. Biochemical typing of scrapie strains. Nature 1997;386:564
54. Lehmann S, Harris DA. Blockade of glycosylation promotes acquisition of scrapie-like properties by the prion protein in cultured cells. J Biol Chem 1997;34:21479–87
55. Taraboulos A, Raeber AJ, Borchelt DR, Serban D, Prusiner SB. Synthesis and trafficking of prion proteins in cultured cells. Mol Biol Cell 1992;3:851–63
56. Caughey B, Raymond GJ. The scrapie-associated form of PrP is made from a cell surface precursor that is both protease- and phospholipase-sensitive. J Biol Chem 1991;266:18217–23
57. Vey M, Pilkuhn S, Wille H, et al. Subcellular colocalization of cellular and scrapie prion proteins in caveolae-like membranous domains. Proc Natl Acad Sci USA 1996;93:14945–49
58. Kreisel W, Volk BA, Buchsel R, Reutter W. Different half-lives of the carbohydrate and protein moieties of a 110,000-dalton glycoprotein isolated from plasma membranes of rat liver. Proc Natl Acad Sci USA 1980;77:1828–31
59. Tauber R, Park CS, Reutter W. Intramolecular heterogeneity of degradation in plasma membrane glycoproteins: Evidence for a general characteristic. Proc Natl Acad Sci USA 1983;80:4026–29
60. McKinley MP, Taraboulos A, Kenaga L, et al. Ultrastructural localization of scrapie prion proteins in secondary lysosomes of infected cultured cells. J Cell Biol 1990;111:316a
61. Tauber R, Kreisel W, Reutter W. Oligosaccharide reprocessing of plasma membrane glycoproteins. In: Conradt HS, ed. Protein glycosylation: Cellular, biotechnological and analytical aspects. Gesellschaft für Biotecnologische Forschung mbH, 1991:21–32
62. Katz SA, Opsahl JA, Abraham PA, Gardner MJ. The relationship between renin isoelectric forms and renin glycoforms. Am J Physiol 1994;267:R244–52
63. Brown DR, Schmidt B, Kretzschmar HA. Role of microglia and host prion protein in neurotoxicity of a prion protein fragment. Nature 1996;380:345–47
64. Raeber AJ, Race RE, Brandner S, et al. Astrocyte-specific expression of hamster prion protein (PrP) renders PrP knockout mice susceptible to hamster scrapie. Embo J 1997;16:6057–65
65. Brown DR, Qin K, Herms JW, et al. The cellular prion protein binds copper in vivo. Nature 1997;390:684–87
66. Stockel J, Safar J, Wallace AC, Cohen FE, Prusiner SB. Prion protein selectively binds copper (II) ions. Biochemistry 1998;37:7185–93
67. Levitt M: ENCAD: Energy calculations and dynamics. Stanford University: Yeda, Rehovot, 1990
68. Levitt M, Hirshberg M, Sharon R, Daggett V. Potential energy function and parameters for simulations of molecular dynamics of proteins and nucleic acids in solution. Comp Phys Commun 1995;91: 215–31

Received January 5, 1999
Revision received May 6, 1999
Accepted May 10, 1999